JACS
JOURNAL OF THE AMERICAN CHEMICAL SOCIETY
Communication
pubs.acs.org/JACS

Polyelectrolyte as Solvent and Reaction Medium

Simon Prescher,[‡] Frank Polzer,[§] Yan Yang,[‡] Miriam Siebenbürger,[⊥] Matthias Ballauff,[⊥] and Jiayin Yuan*[,‡]

[‡]Department of Colloid Chemistry, Max Planck Institute of Colloids and Interfaces, D-14424 Potsdam, Germany
[§]Institute of Physics, Humboldt-Universitaet zu Berlin, D-12489, Berlin, Germany
[⊥]Soft Matter and Functional Materials, Helmholtz-Zentrum Berlin für Materialien und Energie, D-14109 Berlin, Germany

Supporting Information

ABSTRACT: A poly(ionic liquid) with a rather low glass transition temperature of −57°C was synthesized via free radical polymerization of an acrylate-type ionic liquid monomer. It exhibits fluidic behavior in a wide temperature range from room temperature to the threshold of the thermal decomposition. We demonstrate that it could act as a unique type of macromolecular solvent to dissolve various compounds and polymers and separate substances. In addition, this polyelectrolyte could serve successfully as reaction medium for catalysis and colloid particle synthesis. The synergy in the solvation and stabilization properties is a striking character of this polymer to downsize the *in situ* generated particles.

Polyelectrolytes are polymers carrying either positively or negatively charged ionizable groups.[1] In polar solvents such as water, polyelectrolytes adopt an extended coil conformation, resulting from the electrostatic repulsion of neighboring charges.[2] In bulk they are typically solid with a glass transition temperature (T_g) far beyond room temperature (rt), e.g., poly(sodium 2-acrylamido-2-methylpropanesulfonate), $T_g \approx$ 168°C, and poly(acrylic acid) sodium salt, $T_g \approx$ 230°C.[3] For certain polyelectrolytes, e.g., poly(styrene sulfonate) sodium salt, the T_g's might even surpass the thermal decomposition threshold, thus far inaccessible.

Poly(ionic liquid)s (PILs), i.e., polymerized ionic liquids, have been recently recognized as innovative polyelectrolytes.[4] Dense incorporation of ionic liquid (IL) moieties into the macromolecular architecture broadens the window of physical properties of common polyelectrolytes, and consequently expands their function and application spectrum.[5] For example, PILs show good solubility in various solvents of different polarity and hydrophobicity, depending on the cation−anion pair, which can be chosen from a large population in IL chemistry.[6] This solubility rule is also applicable to PIL colloids to transport them into hydrophobic solvents via anion exchange.[7] Combining the adaptable solubility in organic solvents and the superior processability afforded by the polymer nature, PILs are able to form transparent films of different thickness, making them model systems to investigate the bulk nature of polyelectrolytes.[8]

Tunable T_g over a wide range is another prominent PIL characteristic. There have been some previous studies on the intrinsic relationship between structural features and variation in T_g.[9] Generally, high asymmetry and large size of the cation and anion can dramatically weaken the tendency of the opposite charges to coordinate and minimize intermolecular interactions, thus effectively lowering the T_g. Judicious choice of the cation and anion structure therefore will build up a toolbox to design many low-T_g polymers. Considering the generally high thermal stability of polyelectrolytes, this immediately creates a wide temperature range between T_g and the structure-preservation threshold, usually the thermal decomposition temperature. Although the physical properties and chemistry of bulk polyelectrolytes in this temperature regime are of special interest in research, much remains unexplored due to the lack of suitable model systems.[10]

Here we report the synthesis of a low-T_g (−57°C) PIL that possesses a large fluid state window from rt up to its thermal decomposition at 220°C. Within this range, this polyelectrolyte not only is able to dissolve some organic compounds and polymers and separate substances by extraction, but also simultaneously serves as reaction medium and stabilizing agent in catalysis and colloidal particle synthesis, herein exemplified by Pt nanoparticles (NPs) and polystyrene (PS) latex.

Some low-T_g polymers have been previously documented in the literature.[11] It is generally accepted that the absence of polar groups or ion pairs will minimize intermolecular interactions and facilitate the motion of polymer chains at relatively low temperatures. This explains why many low-T_g polymers are nonpolar and hydrophobic, e.g., the polybutadiene or poly(*n*-alkyl acrylate) series. Maskos et al. also studied polyelectrolyte−surfactant complexes with considerably low T_g's.[12] Very recently, several groups showed that, despite high charge density, PILs might reach a low T_g by structurally shielding coulombic interactions and sufficiently plasticizing the polymer backbone.[13] For example, in an elegant report by Snow et al., an IL polymer showed a low T_g of −47°C and consequently an electrowetting effect.[13a] However, its absolute molecular weight and the water content were not given, which leads to debate about whether a low-T_g pure PIL can be truly fluid like an IL near rt.

In the present work, the low-T_g polyelectrolyte was prepared via a modification of Snow's approach, in which a propyl spacer is placed between a polymerizable acrylate head and a distal ion pair of sulfonate−ammonium. Figure 1A depicts the synthetic route to this PIL, named PAAPS. After exhaustive dialysis against water, the oily PIL was dried at 100°C under high vacuum (1×10^{-3} mbar) for 12 h to minimize the water content (<0.2 wt% by Karl−Fischer titration). The weight-averaged absolute molecular

Received: September 14, 2013
Published: December 2, 2013

   dx.doi.org/10.1021/ja409395y | J. Am. Chem. Soc. 2014, 136, 12−15

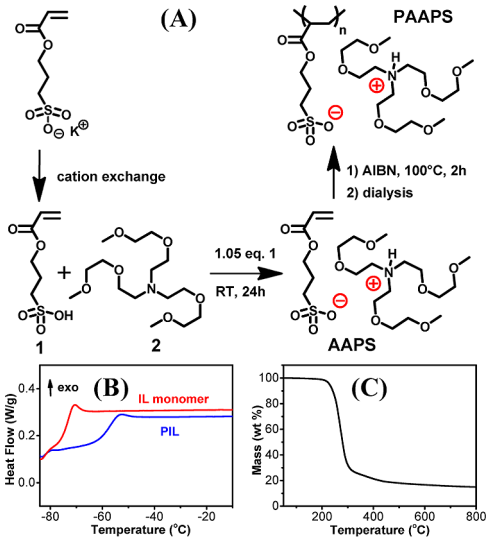

Figure 1. (A) Reaction scheme for the synthesis of a low-T_g PIL, PAAPS. (B) DSC curves of the IL monomer and PIL. (C) TGA curve of the PAAPS PIL.

weight of PAAPS was determined by analytical ultracentrifugation to be 69 kDa, with a polydispersity index of 2.15 (Figure S1).

The T_g's of the IL monomer and PIL were determined by differential scanning calorimetry (DSC, Figure 1B) to be −74 and −57°C, respectively. Thermal gravimetric analysis (TGA, Figure 1C) indicates that the polymer is stable up to 220°C. This defines a temperature window of 280°C from the initial chain motion to the thermal scission. Since the T_g is 80°C below ambient temperature, the fluid behavior triggers our interest. This was first illustrated in a flow experiment, shown in Figures 2

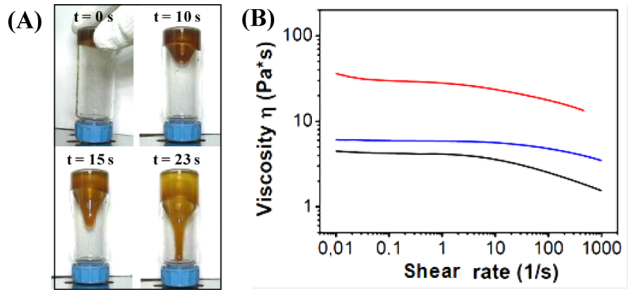

Figure 2. (A) Photographs recording the flow of PAAPS in a sealed upside-down glass vial at 100°C. (B) Viscosity of the AAPS monomer at 25°C (black) and of PAAPS polymer at 100 (red) and 150°C (blue).

and S3. The movement of the polymer along the glass wall was monitored with a digital camera, and the time for the polymer to first reach the bottom cap of the glass vial (8 cm distance) was recorded.

At ambient temperature, the polymer fell rather slowly, taking 70 min to cover the 8 cm distance, indicative of retarded advancing of the bulk polymer along the glass wall (Figure S3). At 60°C, this process was accelerated by a factor of 12, as the polymer flowed to the bottom within 5 min (Figure S3). At 100°C, the polymer presented a typical liquid behavior and started to follow the movement of the glass; i.e., deformation began as soon as the vial was inverted, and the polymer reached the bottom within 23 s (Figure 2A). At an even higher temperature of 150°C, the polymer flowed like common room-temperature ILs. It is worth noting that the colorization of PAAPS is caused by the amine functionality, which turns brown-orange upon heating or long-term storage (Figure S4), though ^{1}H NMR fails to prove any change in its chemical structure.

Quantitative analysis of the rheological behavior of the IL monomer and PIL at different temperatures was done by measuring viscosity under dry air. All measured samples exhibited shear thinning behavior when shear viscosity was plotted vs shear rate (Figure 2B). The AAPS−IL monomer displays a plateau of constant viscosity at 25°C. This plateau, the Newtonian regime, is characterized by zero shear viscosity, which is found to be $\eta_0 = 4.5$ Pa·s. Above a shear rate of 2.5 s^{-1}, the shear thinning regime starts; shear thinning was previously reported for some ILs.[14] Burrell et al.[15] found that, in the case of $(HOEt)_2NH{\cdot}AcOH$, the zero shear viscosity decreased with increasing water content when staying below 1 equiv. The onset of shear thinning stayed constant but could be shifted to higher frequencies by increasing the temperature. Like the monomer, the PAAPS−PIL polymer shows shear thinning at 100 and 150°C. The value of η_0 for the PIL at 100°C is 30 Pa·s, close to that of chocolate syrup at ambient temperature. At 150°C the PIL has $\eta_0 = 6$ Pa·s, close to that of the IL monomer (4.5 Pa·s) at rt. The reduced viscosity of the polymer at elevated temperature is caused by the higher mobility of the chains and segments and is common for bulk polymers. We assume that the same interactions that lead to shear thinning of the monomer should contribute to the shear response of the corresponding polymer, as well.

The organic composition, ionic nature, and fluid behavior of PAAPS below 100°C satisfy the criteria of ILs; thus, this specific PIL can be considered as an IL compound as well. It enriches the toolbox for IL structure design by introducing a macromolecular IL via the PIL concept. Due to the fluid behavior of the PIL, we were interested in whether the bulk polyelectrolyte can be considered as a macromolecular solvent. Therefore, we investigated the mixing of various chemicals at a fixed weight fraction of 5% relative to the PIL. The mixture was homogenized by magnetic stirring for at least 2 h before it was checked by naked eyes and optical microscopy. Heating to 200°C was necessary for some compounds to accelerate the dissolution.

At rt, both hydrophilic (water, ethanol, tetrahydrofuran, and dimethyl sulfoxide) and hydrophobic solvents (dichloromethane and chloroform) were fairly soluble in PAAPS (Tables 1 and S1).

Table 1. Solubility Table of Different Solvent Liquids in PAAPS

solvent	δ^a	soluble?	solvent	δ^a	soluble?
n-hexane	7.24	×	$CHCl_3$	9.21	√
n-heptane	7.4	×	THF	9.52	√
ether	8.18	×	EtOH	12.92	√
toluene	8.91	√[b]	DMSO	12.93	√
benzene	9.15	√[b]			

[a]Hildebrand solubility parameter, in $kcal^{1/2}/cm^{3/2}$. [b]Only above 50°C.

Toluene and benzene began to solubilize at 50°C. In fact, the aforementioned solvents are miscible with PAAPS at any ratio, pointing to an amphiphilic character of this polyelectrolyte. Interestingly, hydrophobic solvents with a solubility parameter <8.9, e.g., *n*-hexane, *n*-heptane, and ether, are immiscible with PAAPS up to their boiling temperature. Beside solvents, some organic compounds were tested for solubility in PAAPS as well. For instance, 4,4-bipyridine, naphthalene, and glucose were found to dissolve at 100°C, and mannose at 150°C. In contrast,

dx.doi.org/10.1021/ja409395y | J. Am. Chem. Soc. 2014, 136, 12−15

neutral red and β-cyclodextrin are immiscible in PIL even up to 200°C. Nonionic elements, e.g., bromine, iodine, selenium, phosphorus, and sulfur, are generally immiscible with PAAPS, presumably because of their lack of a specific attractive interaction with the polymer structure. The dissolution properties of organic solvents and compounds in PAAPS can be applied for substance separation. As shown in Figure 3, Nile Red and indigo can be readily extracted from their heptane solutions by PAAPS via a heating/shaking/cooling cycle.

Figure 3. Extraction of Nile Red (A) and indigo (B) from their heptane solutions by PAAPS (the bottom phase). Their concentrations are 3.3×10^{-5} and 0.33 mg/mL, respectively.

Apart from low-molecular-weight compounds, polymers were tested for their ability to form a homogeneous polymer blend. Some neutral polymers/oligomers or anionic polyelectrolytes of relatively low molecular weight are readily soluble in PIL, e.g., poly(acrylic acid) (2 kDa) and poly(ethylene glycol) (750 Da). The dissolution usually takes place at elevated temperatures, at which the polymer chain motion is significantly pronounced. In the case of polymers with high molecular weight, the dissolution process is kinetically hampered, so they can be considered as immiscible. This problem can be tackled by employing a common solvent. For example, a poly(ethylene oxide) (1.9 kDa) solution in chloroform (10 wt%) was added to the PIL under mechanical stirring. A stable homogeneous solution was obtained when chloroform was completely removed at 100°C under high vacuum. Cationic polyelectrolytes independent of temperature and molecular weight are overall insoluble due to inter-polyelectrolyte complex formation.

It should be noted that dissolution typically comprises diffusion of solvent molecules into the solid matrix and sequential solvation of the guest molecules in the solvent environment. Apparently, in the current study, the diffusion of a polymeric molecule is significantly more difficult than that of small solvent molecules due to its high molar weight. Furthermore, to afford diffusion in a fluid state, the PIL chains under shear force might be partially oriented, a state that is thermodynamically unfavorable. In addition, for low-molecular-weight solvents, the solvation proceeds by polarizing the guest molecules and capturing the guest molecule in a shell of many solvent molecules. A single polymer chain might be able to solvate a single guest molecule completely by itself or even simultaneously participate in solvation of several guest molecules. Finally, chain entanglement is an intrinsic polymer characteristic that is unavoidable and affects the dissolution process. The physical entanglement of the polymer chains absent in common solvents can occur and hamper the motion and solvation process. All these factors indicate that dissolution of solutes in a PIL might involve many issues.

Many chemical reactions require solvents for dilution, reaction homogenization, and heat/mass transfer. The observed fluid behavior and the solubilization property of the low-T_g PIL make it possible to apply PILs as reaction media for materials synthesis. As a proof of concept, we conducted two model experiments: the synthesis of Pt NPs and the emulsion polymerization of styrene.

For the synthesis of Pt NPs, H_2PtCl_6 was employed as the metal source (0.25 wt% relative to the polymer) and ethylene glycol as the reducing agent (0.75 wt%). A homogeneous dispersion of NPs was obtained at 150 °C. Figure 4A is a typical

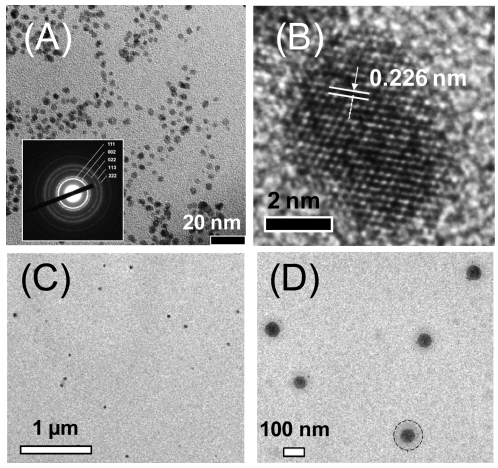

Figure 4. TEM bright-field images. (A) Pt NPs synthesized in PIL at 150°C. Inset: the corresponding SAED pattern indicating a cubic close-packed crystal structure. (B) HRTEM image of a single Pt NP with a lattice plane distance of 0.226 nm, corresponding to the (111) lattice plane. (C) PS latex prepared via emulsion polymerization of styrene in PAAPS at 100°C and (D) enlarged view. The dashed circle indicates the border of the PIL brush on the PS latex surface.

transmission electron microscopy (TEM) image of the as-prepared Pt NPs. Well-dispersed Pt NPs with an average size of 3.5 ± 0.4 nm were clearly visible. Selected area electron diffraction (SAED, inset in Figure 4A) of the NPs presents characteristic diffraction patterns that can be indexed to the (111), (002), (022), (113), and (222) lattice planes of the Pt NPs, indicating a cubic close-packed crystal structure. The HRTEM (high-resolution TEM) image in Figure 4B visualizes the *d*-spacing of the (111) plane expanding throughout the entire NP. This finding proves that, even at high temperatures, highly dispersible and stable single-crystalline Pt NPs can be produced by applying a fluid bulk PIL as reaction medium. The catalytic activity of the as-synthesized Pt NPs in bulk PAAPS is exemplified (Table S2) by a model reaction, hydrogenation of nitroaromatics. It is inspiring that both hydrophilic and hydrophobic substrates performed well when this PAAPS−Pt system was used as both catalyst and solvent. Here PAAPS shows an amphiphilic nature, strong stabilizing power, and solvation function in this catalysis model running at high temperature. This property is highly desired in catalysis, yet hardly achievable from normal solvents.

In the case of emulsion polymerization of styrene, the monomer (10 wt% relative to the PIL) and the thermal initiator AIBN (5 wt% relative to styrene) were mixed with PIL at rt. The polymerization was performed without any stabilizer at 100°C for 2 h under nitrogen atmosphere with mechanical stirring. A homogeneous latex dispersion formed shortly after the reaction started. The ^{1}H NMR spectrum of the reaction mixture proves that styrene was polymerized completely in 2 h. The PS latex dispersion was stable in water and was subjected to TEM characterization. As shown in Figure 4, some PS latexes are evenly distributed on the carbon-coated copper TEM grid,

dx.doi.org/10.1021/ja409395y | J. Am. Chem. Soc. 2014, 136, 12−15

possibly because the PAAPS chains preferentially stick to the carbon surface. This PAAPS−carbon interaction can be proven by stabilization of single-walled carbon nanotubes in bulk PAAPS, as detailed in Figure S5. Some PS latexes are also observed in an aggregation state due to a "coffee ring" phenomenon on the TEM grid (Figure S6). A statistical calculation reveals that the PS latex has an average size of 75 nm, with a size deviation of 10 nm (Figure S9).

In both dispersion systems of Pt NPs and PS lattices, the as-synthesized colloids were fairly soluble in various solvents that can dissolve PAAPS. For example, Pt NPs can be transferred not only to water and acetone but also to benzene and chloroform. This solubility character hints that the PIL chains seem to stick to the colloidal particle surface and stabilize them in solvents. A close view of the PS latex in the TEM image (Figure 4D, highlighted by a dashed circle) reveals a dark corona which was frequently observed around individual latex particles. Further characterization with dynamic light scattering shows an average size of 115 ± 5 nm for the latex dispersion (Figure S10), indicating a PIL grafting layer of, on average, 20 nm on the PS latex surface in solution state. This hypothesis is further proven by Fourier transform infrared (FTIR) spectroscopy measurements of the pure PS, PIL, and the purified PS latex prepared in PAAPS. As shown in the Supporting Information, the FTIR curve of PS latex exhibits characteristic bands from both PS and PAAPS, demonstrating that the PIL molecules coexist with the PS latex in the final colloidal product. Combining the solubility behavior and the FTIR characterization, it is deduced that the PIL chains were attached to the colloidal surface during the particle formation. The PIL acts not only as a reaction medium but also as a powerful stabilizer to spontaneously down-size the *in situ* generated particles.

In summary, we present the synthesis, fluid behavior, and application of a low-T_g PIL (−57°C) as solvent for substance dissolution and separation, and reaction medium for catalysis and colloidal synthesis. The PIL's viscosity largely depends on the temperature. Although it flows rather slowly at room temperature, its liquid character becomes more pronounced at elevated temperatures, at which many reactions can be applied. The synthetic approach using PIL as a reaction medium shown for Pt nanoparticles and PS latex is applicable for a broad range of colloid systems. Apart from the synthesis of particles and catalysis, other chemical reactions like organic synthesis and solution polymerizations might also be possible using such a low-T_g PIL approach. This work thus points out the great potential of liquid polyelectrolytes as solvents in many different reaction systems.

■ ASSOCIATED CONTENT

Supporting Information

Materials, synthesis, and some characterizations. This material is available free of charge via the Internet at http://pubs.acs.org.

■ AUTHOR INFORMATION

Corresponding Author

jiayin.yuan@mpikg.mpg.de

Notes

The authors declare no competing financial interest.

■ ACKNOWLEDGMENTS

The authors thank the Max Planck Society for the financial support. We thank Prof. Markus Antonietti, Dr. Klaus Tauer, and Dr. Tristan Corbiere for helpful discussions. S.P. thanks Antje Voelkel for the AUC measurements. F.P. thanks the CRC 951 of the Deutsche Forschungsgemeinschaft and the Joint Lab for Structural Research Berlin for funding.

■ REFERENCES

(1) Dobrynin, A. V.; Rubinstein, M. *Prog. Polym. Sci.* **2005**, *30*, 1049.

(2) (a) Ballauff, M.; Borisov, O. *Curr. Opin. Colloid Interface Sci.* **2006**, *11*, 316. (b) Wittemann, A.; Drechsler, M.; Talmon, Y.; Ballauff, M. *J. Am. Chem. Soc.* **2005**, *127*, 9688.

(3) Yeo, S. C.; Eisenberg, A. *J. Macromol. Sci. Part B* **1977**, *13*, 441.

(4) (a) Green, M. D.; Long, T. E. *Polym. Rev.* **2009**, *49*, 291. (b) Green, O.; Grubjesic, S.; Lee, S.; Firestone, M. A. *Polym. Rev.* **2009**, *49*, 339. (c) Yuan, J.; Mecerreyes, D.; Antonietti, M. *Prog. Polym. Sci.* **2013**, *38*, 1009. (d) Mecerreyes, D. *Prog. Polym. Sci.* **2011**, *36*, 1629. (e) Yuan, J.; Antonietti, M. *Polymer* **2011**, *52*, 1469. (f) Ye, Y.; Choi, J.-H.; Winey, K. I.; Elabd, Y. A. *Macromolecules* **2012**, *45*, 7027. (g) Hemp, S. T.; Allen, M. H.; Green, M. D.; Long, T. E. *Biomacromolecules* **2011**, *13*, 231. (h) Hu, X.; Huang, J.; Zhang, W.; Li, M.; Tao, C.; Li, G. *Adv. Mater.* **2008**, *20*, 4074. (i) He, H.; Zhong, M.; Adzima, B.; Luebke, D.; Nulwala, H.; Matyjaszewski, K. *J. Am. Chem. Soc.* **2013**, *135*, 4227. (j) Choi, U. H.; Mittal, A.; Price, T. L.; Gibson, H. W.; Runt, J.; Colby, R. H. *Macromolecules* **2013**, *46*, 1175. (k) Lee, M.; Choi, U. H.; Colby, R. H.; Gibson, H. W. *Chem. Mater.* **2010**, *22*, 5814. (l) Choi, U. H.; Lee, M.; Wang, S.; Liu, W.; Winey, K. I.; Gibson, H. W.; Colby, R. H. *Macromolecules* **2012**, *45*, 3974.

(5) (a) Zhao, L.; Crombez, R.; Caballero, F. P.; Antonietti, M.; Texter, J.; Titirici, M.-M. *Polymer* **2010**, *51*, 4540. (b) Antonietti, M.; Shen, Y.; Nakanishi, T.; Manuelian, M.; Campbell, R.; Gwee, L.; Elabd, Y. A.; Tambe, N.; Crombez, R.; Texter, J. *ACS Appl. Mater. Interfaces* **2010**, *2*, 649. (c) England, D.; Tambe, N.; Texter, J. *ACS Macro Lett.* **2012**, *1*, 310. (d) Coupillaud, P.; Pinaud, J.; Guidolin, N.; Vignolle, J.; Fèvre, M.; Veaudecrenne, E.; Mecerreyes, D.; Taton, D. *J. Polym. Sci., Part A: Polym. Chem.* **2013**, *51*, 4530. (e) Pinaud, J.; Vignolle, J.; Gnanou, Y.; Taton, D. *Macromolecules* **2011**, *44*, 1900. (f) Ye, Y.; Sharick, S.; Davis, E. M.; Winey, K. I.; Elabd, Y. A. *ACS Macro Lett.* **2013**, *2*, 575. (g) Chen, X.; Li, Q.; Zhao, J.; Qiu, L.; Zhang, Y.; Sun, B.; Yan, F. *J. Power Sources* **2012**, *207*, 216. (h) Tauer, K.; Weber, N.; Texter, J. *Chem. Commun.* **2009**, 6065. (i) Allen, M. H.; Wang, S.; Hemp, S. T.; Chen, Y.; Madsen, L. A.; Winey, K. I.; Long, T. E. *Macromolecules* **2013**, *46*, 3037. (j) Cheng, S.; Beyer, F. L.; Mather, B. D.; Moore, R. B.; Long, T. E. *Macromolecules* **2011**, *44*, 6509. (k) la Cruz, D. S.-d.; Green, M. D.; Ye, Y.; Elabd, Y. A.; Long, T. E.; Winey, K. I. *J. Polym. Sci. Part A: Polym. Phys.* **2012**, *50*, 338.

(6) Marcilla, R.; Blazquez, J. A.; Fernandez, R.; Grande, H.; Pomposo, J. A.; Mecerreyes, D. *Macromol. Chem. Phys.* **2005**, *206*, 299.

(7) Yuan, J.; Antonietti, M. *Macromolecules* **2011**, *44*, 744.

(8) (a) Nakamura, K.; Saiwaki, T.; Fukao, K.; Inoue, T. *Macromolecules* **2012**, *44*, 7719. (b) Nakamura, K.; Fukao, K.; Inoue, T. *Macromolecules* **2011**, *45*, 3850.

(9) Ohno, H. *Macromol. Symp.* **2007**, *249−250*, 551.

(10) Tollan, C. M.; Marcilla, R.; Pomposo, J. A.; Rodriguez, J.; Aizpurua, J.; Molina, J.; Mecerreyes, D. *ACS Appl. Mater. Interfaces* **2008**, *1*, 348.

(11) (a) Narh, K. A. *Adv. Polym. Technol.* **1996**, *15*, 245. (b) Boyce, R. J.; Bauer, W. H.; Collins, E. A. *Trans. Soc. Rheol.* **1966**, *10*, 545.

(12) (a) Antonietti, M.; Maskos, M. *Macromolecules* **1996**, *29*, 4199. (b) Antonietti, M.; Maskos, M. *Macromol. Rapid Commun.* **1995**, *16*, 763. (c) Antonietti, M.; Maskos, M.; Kremer, F.; Blum, G. *Acta Polym.* **1996**, *47*, 460.

(13) (a) Ricks-Laskoski, H. L.; Snow, A. W. *J. Am. Chem. Soc.* **2006**, *128*, 12402. (b) Washiro, S.; Yoshizawa, M.; Nakajima, H.; Ohno, H. *Polymer* **2004**, *45*, 1577.

(14) Amann, T.; Dold, C.; Kailer, A. *Soft Matter* **2012**, *8*, 9840.

(15) Burrell, G. L.; Dunlop, N. F.; Separovic, F. *Soft Matter* **2010**, *6*, 2080.